Int J Thermophys (2010) 31:1964–1971
DOI 10.1007/s10765-009-0564-8

Control of Optical Performance in Infrared Region for Vanadium Dioxide Films Layered by Amorphous Silicon

H. Kakiuchida · P. Jin · M. Tazawa

Published online: 5 March 2009

Abstract The multilayer structure of amorphous silicon (*a*-Si) with vanadium dioxide (VO_2) that possesses excellent thermochromism in the infrared range was formed by reactive magnetron sputtering. Then, the physical properties such as thermochromic performance, crystalline structure, and film morphology were investigated. As a result, the *a*-Si layer was found to flexibly control the optical-spectral variation due to thermochromism produced in the VO_2 layer over a wide infrared range. The multilayer structure of VO_2 between *a*-Si layers is an effective way to design various infrared thermochromic devices, since the refractive index of *a*-Si can be widely varied by oxidation.

Keywords Amorphous silicon · Infrared radiation control · Magnetron sputtering · Semiconductive-to-metallic phase transition · Thermochromism · Vanadium dioxide

1 Introduction

Vanadium dioxide (VO_2), which exhibits a semiconductor-to-metal phase transition, has excellent thermochromic performance, that is, a large variation in optical constants particularly at near-infrared and longer wavelengths [1,2]. Since the transition temperature is at approximately 68 °C, and additionally it can be reduced to the vicinity of room temperature by a trace of dopant [3,4], such thermochromic function is applicable to solar-radiation control for seasonably comfortable houses [5]. In summer, the intensity of solar radiation into a room through a window decreases, while it increases

H. Kakiuchida (✉) · P. Jin · M. Tazawa
Materials Research Institute for Sustainable Development, National Institute for Advanced Industrial Science and Technology (AIST), 2266-98 Anagahora, Shimoshidami, Moriyama, Nagoya 463-8560, Japan
e-mail: h.kakiuchida@aist.go.jp

in winter. Since the transmittance of VO_2 is controlled automatically by a variation in ambient temperature due to seasonal changes, no switching devices are needed.

Optical spectra for the low- and high-temperature phases of VO_2, which correspond to semiconductive and metallic phases, respectively, are still desired to be more highly controllable at infrared wavelengths. We have earlier proposed several multilayer structures composed of VO_2 and transparent materials such as TiO_2, ZrO_2, etc. [5,6]. However, the refractive index of VO_2 is so large that optical materials with a higher refractive index, preferably over three, are desired when they are layered with VO_2 for better controlling the spectral change due to thermochromism.

This study focuses on the multilayer structure of amorphous silicon (*a*-Si) with VO_2 film, because *a*-Si film has several advantages: (i) refractive index higher than that of VO_2, (ii) high controllability of refractive index by oxidation [7], and (iii) manageability in deposition technique and cost. From the viewpoint of practical fabrication of this multilayer structure, material suitability of *a*-Si film for VO_2 film is indispensable. The under- (over-)coatings of the VO_2 layer by amorphous materials may affect the physical properties of VO_2 such as the stability of crystalline growth, film morphology, and thermochromic functionality, because the crystalline structure of the vanadium-oxide system (VO_n: $0 < n < 2.5$) [8] is sensitive to under- (over-)coated materials. For example, Muraoka et al. [9] have examined the electrical-resistance variation due to the phase transition of VO_2 film deposited on a TiO_2 substrate with various crystal faces, and then they have reported the correlation between the phase-transition temperature and lattice parameter of VO_2. On the other hand, Kato et al. [10] have shown that the phase-transition behavior is strongly affected by the thickness of a zinc oxide (ZnO) layer as an undercoat of VO_2 film. According to the previous results, the phase transition or thermochromism strongly depends on the lattice (mis)match with crystalline materials under the VO_2 film. Thus, the potential of amorphous materials for stable deposition of VO_2 film is considerable, since the amorphous structure has no specific crystal lattice.

In this study, the feasibility to layer VO_2 film with *a*-Si film was studied with regard to material suitability and optical design. By using radio frequency (rf)-reactive magnetron sputtering, which can possibly disturb the stability of VO_2 crystalline growth but must be used for practical reasons, the multilayer structure composed of VO_2 film sandwiched by a pair of *a*-Si layers (SVS structure) was formed, and then the crystalline structure, film morphology, and optical properties of VO_2 and *a*-Si were investigated.

2 Experimental and Estimation Procedures

The films were deposited by rf-reactive magnetron sputtering using metal targets. VO_2 film was deposited by sputtering a vanadium (V) target in argon (Ar) and oxygen (O_2) gases under flow rates of 32 sccm and 1.8 sccm, respectively, with a total pressure of 0.6 Pa, rf power of 100 W, and substrate temperature of 600 °C. On the other hand, *a*-Si film was deposited by sputtering a silicon (Si) target in Ar gas at a flow rate of 32 sccm, 0.6 Pa in total pressure, 120 W in rf power, and 600 °C in substrate temperature. Before sputtering was initiated, the vacuum chamber was evacuated to 2×10^{-6} Pa. The VO_2

films sandwiched by a pair of *a*-Si layers (SVS structure) at several thicknesses, which have the effect of controlling the optical spectrum, were designed as optical multilayers by coordination of the sputtering procedure.

To determine the optical constants and deposition rates of the present VO_2 and a-SiO_x films, single-layered samples had been preliminarily prepared and the thickness and optical constants were analyzed by conventional ellipsometry. The measurements were carried out using an ellipsometer (J. A. Woolam Co., Inc., M2000).

The thermochromic behavior of the VO_2 film between *a*-Si layers was examined at visible and near-infrared wavelengths by a spectrophotometer (Hitachi High-Technologies Corp., U4100), and at infrared wavelengths by an FTIR (Perkin Elmer Inc., GX1P). The morphology of the SVS structure was observed by a scanning electron microscope (SEM) (Hitachi High-Technologies Corp., S-4300) and an atomic force microscope (AFM) (Veeco Instruments Inc., MultiMode). The crystalline information was obtained by X-ray diffractometry (XRD) in the θ–2θ mode with CuK_α (Rigaku Corp., RINT2000).

3 Estimation, Results, and Discussion

Figure 1 shows the optical constants of a-SiO_x films prepared by reactive sputtering of a silicon target in various O_2 atmospheres, where the other sputtering conditions were the same as in *a*-Si deposition. The reported data for *a*-Si and a-SiO_2 are also plotted in the figure [11,12]. The insets show near-infrared optical constants plotted against the flow rate of O_2 during the sputtering process. The right-hand ordinate of the inset in Fig. 1a indicates the oxidation number, x, which was estimated through the

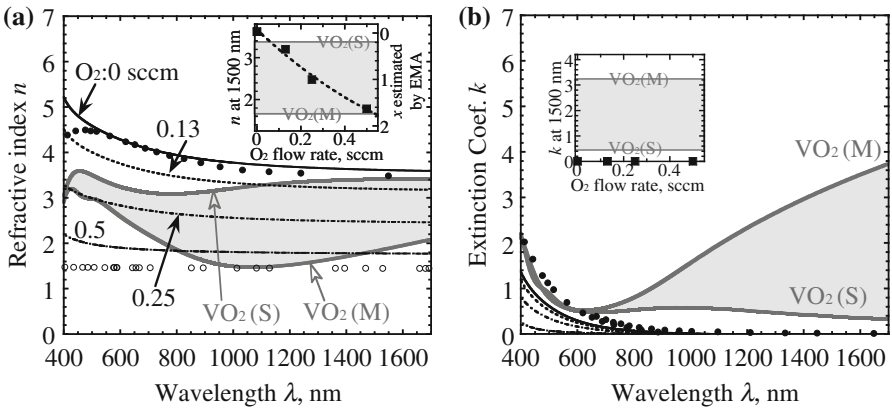

Fig. 1 Optical constants of a-SiO_x (*black curves*), deposited by sputtering a Si target at various O_2 flow rates, where *closed* and *open circles* represent the reported values of *a*-Si and a-SiO_2, respectively [11,12]. *Insets* show the optical constants and oxidation number of a-SiO_x at a wavelength of 1500 nm as a function of O_2 flow rate, where x was estimated by EMA from the optical constants of *a*-Si and a-SiO_2, as detailed in the text. The values of VO_2 change reversibly with temperature by a semiconductive-to-metallic (S-to-M) phase transition, as expressed by *gray curves* and *areas*, where the values of S and M phases were measured at 30 °C and 90 °C, respectively

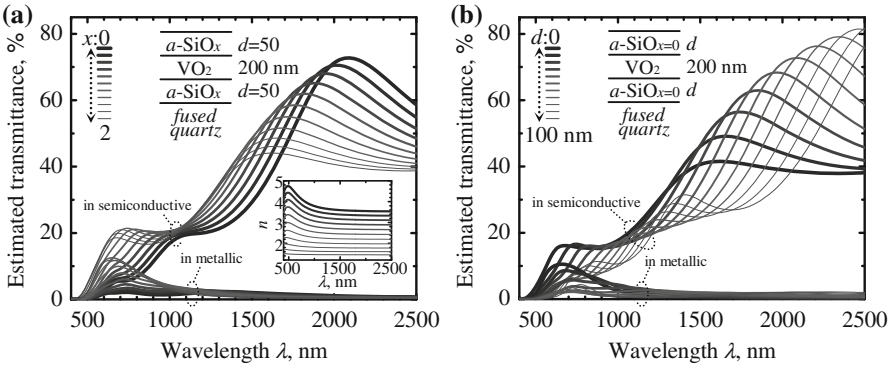

Fig. 2 Optical transmittances of SVS structures on fused quartz at various (**a**) oxidation numbers, x, and (**b**) thicknesses of a-SiO_x layers, d, which were estimated from optical constants of semiconductive and metallic VO_2 and a-SiO_x, as shown in Fig. 1. The transmittances were simulated by using refractive indices of a-SiO_x at several x as shown in the *inset*, and those of VO_2 (S and M) as shown in Fig. 1. The layer structures are schematically shown in the figures

Bruggeman effective medium approximation (EMA) [13] from the reported optical constants of a-Si and a-SiO_2. The refractive index of a-SiO_x decreases monotonically with an increase in the flow rate of O_2, and it covers the values of both semiconductive and metallic VO_2. On the other hand, the extinction coefficient of a-SiO_x is approximately zero in the near-infrared range, although a shoulder of the optical absorption edge appears. This suggests high controllability of thermochromic behavior by introduction of a-SiO_x layers multilayered with VO_2. For example, the transmittance spectra of an SVS structure including a 200 nm thick VO_2 layer were estimated from the optical constants of VO_2 and a-SiO_x, as shown in Fig. 2a, b. The refractive indices of a-SiO_x used for the transmittance estimations are shown as the inset in Fig. 2a, which were obtained by the aforementioned EMA. Particularly in the near-infrared range, the transmittance change due to thermochromism produced in the VO_2 layer is well controlled by the thickness and/or oxidation number of a-SiO_x layers.

Figure 3a, b show SEM images of cross sections of the VO_2 single- and SVS multilayers on a fused-quartz substrate, respectively. The insets show close-up views of their morphologies as measured by AFM. Crystalline-like grains with submicron size appear in both samples. The grains observed in the SVS multi-layer sample (Fig. 3b) are, on the average, smaller and more closely packed than those in the VO_2 single-layer sample (Fig. 3a). Figure 3c shows XRD patterns of the VO_2 single- and SVS multilayers on a fused-quartz substrate in the range between 20° and 60° in 2θ, where solid bars at the bottom of the graphs are the peaks identified by crystalline VO_2 [14]. The peak at around 28° in 2θ, which corresponds to (011) interplanar spacing of monoclinic VO_2, appears in both samples. The peak intensity seems to be larger in the SVS structure than in the VO_2 single layer. The information for the film morphology and crystalline quality, as aforementioned, suggests that VO_2 can be formed even in the SVS structure and an a-Si layer does not decrease the stability of the VO_2 formation.

Since a-Si has a large refractive index and a small extinction coefficient at near-infrared wavelengths, the SVS structure is expected to provide excellent controllability

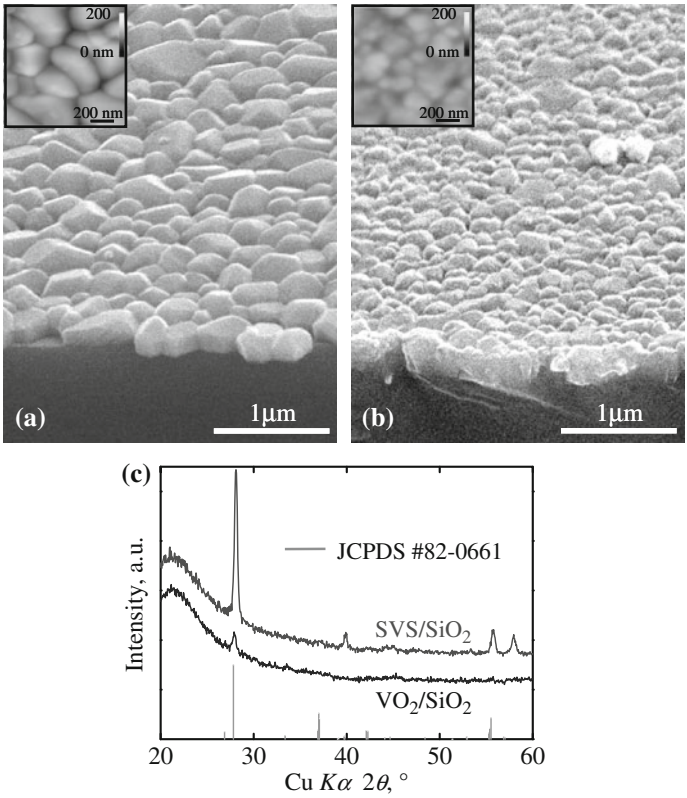

Fig. 3 SEM images of cross sections of (**a**) VO_2 single- and (**b**) SVS multilayer films on fused quartz. *Insets* show surface configurations measured by AFM, and **c** XRD patterns, where the peak around 28° is attributed to (011) monoclinic VO_2 [14]

of the change in the optical spectrum due to thermochromism of VO_2. The transmittance (T) and reflectance (R) of VO_2 single- and SVS multi-layers with different thicknesses on the fused-quartz substrate are plotted against wavelength in Fig. 4a–d. R at a wavelength of 1500 nm is plotted against temperature in the insets in Fig. 4b, d. The layer structures are schematically shown in the respective figures. For T and R measurements, the angles of incidence are 0° and 20°, respectively, as schematically shown in Fig. 4a, and the incident light was unpolarized and the detected light was not selective with regard to polarization. As a whole, thermochromic performance clearly appears in both VO_2 single- and SVS multi-layer samples, which bears direct evidence from the viewpoint of optical performance: the *a*-Si layer does not result in a decline of the crystalline quality of VO_2 and consequent thermochromism. The changes in T and R due to thermochromism seem to be marked rather in the near-infrared range. While the optical spectra are simple for the VO_2 single-layer structure, as shown in Fig. 4a, b, the optical spectra are drastically transfigured by the sandwich of VO_2 by *a*-Si layers, as shown in Fig. 4c, d. The changes in transmittance and reflectance due to thermochromism around specific wavelengths can be flexibly expanded or reduced.

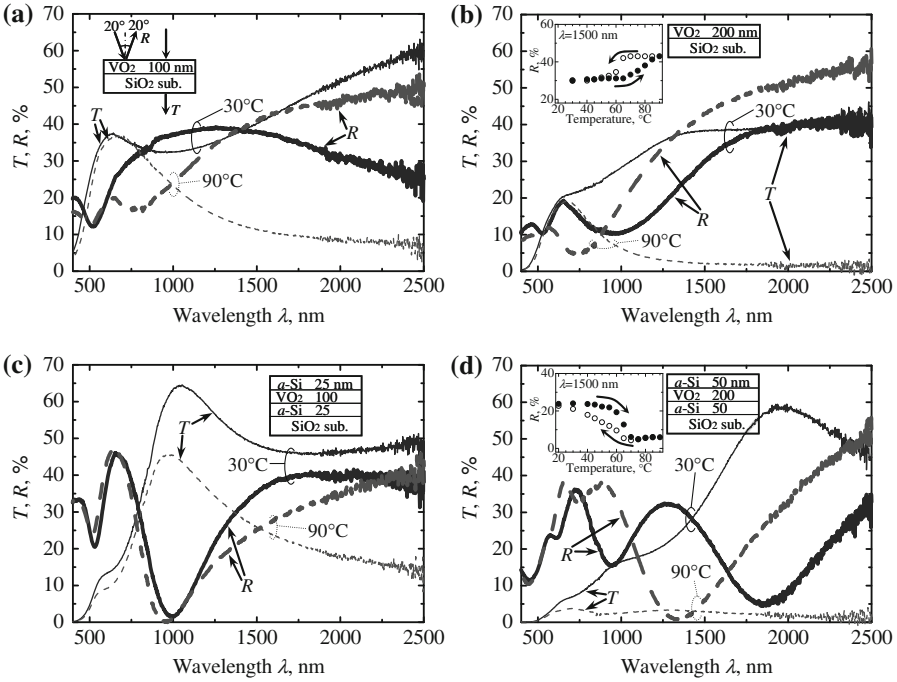

Fig. 4 Transmittance (T) and reflectance (R) spectra of various film structures including thermochromic VO_2 layer, where the layer structures are schematically shown in the respective figures. T and R were measured for semiconductive (30 °C) and metallic (90 °C) phases of VO_2. R at a wavelength of 1.5 μm is plotted against temperature in (**b**) and (**d**). *Insets* show the reflectance at a wavelength of 1500 nm against temperature, where the *closed* and *open circles* are the results measured in rise and drop in temperature, respectively. The kinks in the spectra at 850 nm result from the change of detectors between visible and infrared ranges

However, these measured spectra deviate from the expected ones as shown in Fig. 2. To discuss the origin of these deviations, the SVS multilayer structure whose spectra are shown in Fig. 4d was ellipsometrically analyzed. Figure 5a shows transmittance (T) and reflectance (R) spectra together with the simulations from the ellipsometric analyses. The analyzed multilayer structure is shown in the same figure. In the present analyses, the EMA layer composed of *a*-Si/void mixture was employed for expressing the rough surface of the top *a*-Si layer [15], which was modeled on the basis of the observed cross section of the film as shown in Fig. 3b. The measured ellipsometric parameters (Ψ, Δ) at both 30 °C and 90 °C agree with the fits, as shown in Fig. 5b, c, respectively, and the measured T and R were consistently reproduced by the present analyses, as shown in Fig. 5a. Accordingly, the top *a*-Si layer possesses an uneven surface of 39 nm in thickness, which is different from the designed layer, while the VO_2 and bottom *a*-Si layers are ideally formed. Therefore, such large surface roughness of the top *a*-Si layer is regarded as the origin of deviation of the measured transmittances from the designed ones.

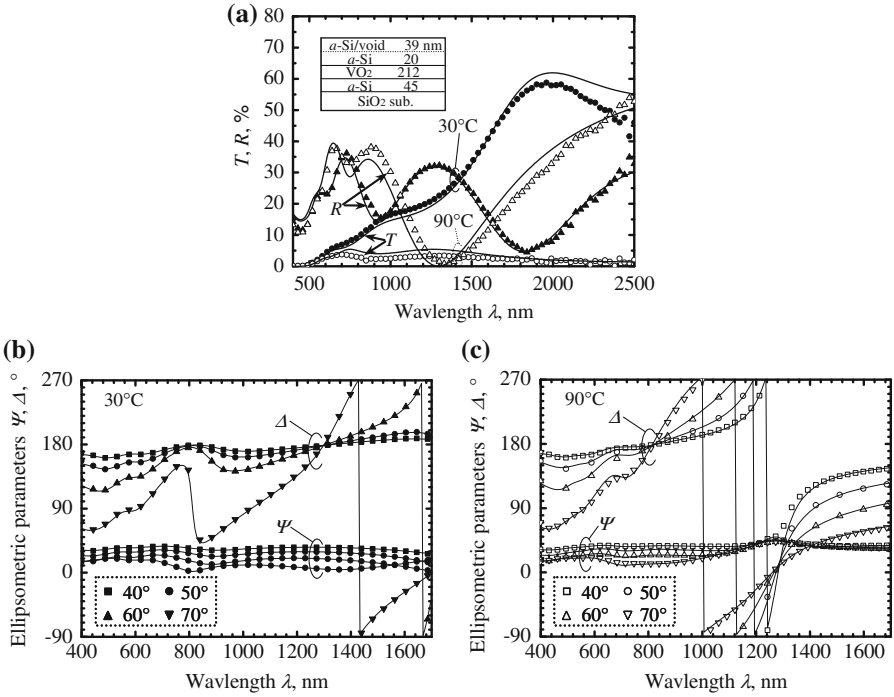

Fig. 5 Transmittance (T), reflectance (R), and ellipsometric parameters (Ψ, Δ) of SVS multi-layer structure at 30 °C and 90 °C. (**a**) T and R reproduced from Fig. 4d, as indicated by closed (30 °C) and open (90 °C) *symbols*. *Inset* shows film structure analyzed by ellipsometry. *Solid curves* are the simulated spectra from the ellipsometric analysis, and (**b**) and (**c**) ellipsometric parameters at 30 °C and 90 °C, respectively. *Symbols* and *solid curves* represent the measurements and fits, respectively. Ψ and Δ were measured at angles of incidence of 40°, 50°, 60°, and 70°

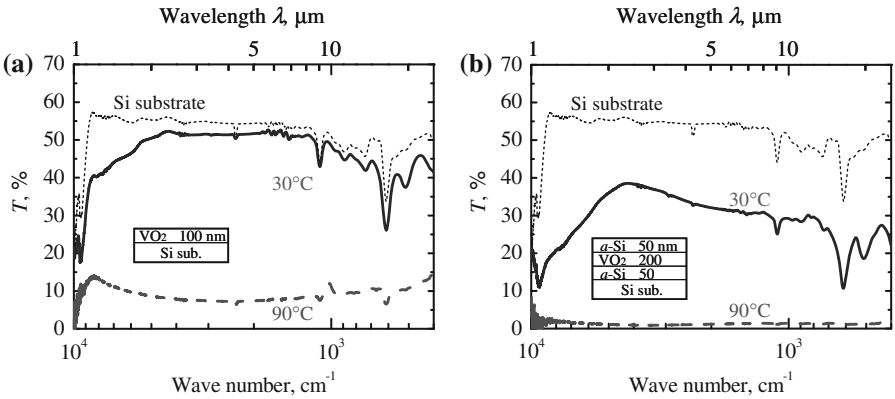

Fig. 6 Infrared transmittance spectra of (**a**) VO_2 single- and (**b**) SVS multilayers on crystalline silicon substrate, where the layer structures are schematically shown in the figures. Note that the spectra contain several absorptions due to vibrational modes of extrinsic materials such as H_2O, CO_2, organic compounds, etc. Transmittances were measured for semiconductive (30 °C) and metallic (90 °C) phases of VO_2

Transmittances of VO_2 single- and SVS multilayer samples at longer wavelengths in the infrared range are shown in Fig. 6a, b. For transmittance measurements in the far-infrared range, crystalline silicon was chosen as a substrate instead of fused quartz. Although the optical design of the present films was not specifically optimized for the far-infrared range, the results exhibit large potential for controlling thermochromic performance in the far-infrared spectrum as well as in the near-infrared region by formation of the appropriate SVS structure.

4 Conclusions

This study demonstrated that layering *a*-Si with VO_2 is an efficient and reliable technique for controlling the change in optical spectrum due to thermochromism at near- and far-infrared wavelengths. In particular, the sandwich structure of VO_2 between *a*-Si layers is an effective way for extending the application range of thermochromic devices, since the refractive index and thickness of the *a*-Si film are highly controllable.

References

1. F.J. Morin, Phys. Rev. Lett. **3**, 34 (1959)
2. J.B. Goodenough, J. Solid State Chem. **3**, 490 (1971)
3. I. Takahashi, M. Hibino, T. Kudo, Jpn. J. Appl. Phys. **40**, 1391 (2001)
4. C.G. Granqvist, Sol. Energy Mater. Sol. Cells **91**, 1529 (2007)
5. P. Jin, G. Xu, M. Tazawa, K. Yoshimura, Appl. Phys. A **77**, 455 (2003)
6. G. Xu, P. Jin, M. Tazawa, K. Yoshimura, Sol. Energy Mater. Sol. Cells **83**, 29 (2004)
7. E. Dehan, P. Temple-Boyer, R. Henda, J.J. Pedroviejo, E. Scheid, Thin Solid Films **266**, 14 (1995)
8. C.H. Griffiths, H.K. Eastwood, J. Appl. Phys. **45**, 2201 (1974)
9. Y. Muraoka, Z. Hiroi, Appl. Phys. Lett. **80**, 583 (2002)
10. K. Kato, P. K. Song, H. Odaka, Y. Shigesato, Jpn. J. Appl. Phys. **42**, 6523 (2003)
11. H. Piller, *in Handbook of Optical Constants of Solids*, ed. by E. D. Palik (Academic Press, San Diego, 1998), pp. 571–586
12. I.H. Mallitson, J. Opt. Soc. Am. **55**, 1205 (1965)
13. D.E. Aspnes, Thin Solid Films **89**, 249 (1982)
14. JCPDS #82–0661
15. H. Fujiwara, J. Koh, P.I. Rovira, R.W. Collins, Phys. Rev. B **61**, 10832 (2000)